Journal of Molecular Graphics and Modelling 39 (2013) 23–28

Contents lists available at SciVerse ScienceDirect

Journal of Molecular Graphics and Modelling

journal homepage: www.elsevier.com/locate/JMGM

Theoretical studies on the common catalytic mechanism of transketolase by using simplified models

Xiang Sheng[a], Yongjun Liu[a,b,*], Chengbu Liu[a]

[a] School of Chemistry and Chemical Engineering, Shandong University, Jinan, Shandong 250100, China
[b] Key Laboratory of Adaptation and Evolution of Plateau Biota, Northwest Institute of Plateau Biology, Chinese Academy of Sciences, Xining, Qinghai 810001, China

ARTICLE INFO

Article history:
Received 19 August 2012
Received in revised form 12 October 2012
Accepted 1 November 2012
Available online 10 November 2012

Keywords:
Transketolase
Density functional theory (DFT) method
Reaction mechanism
ThDP-dependent enzyme
2-Carbon fragment transfer

ABSTRACT

Transketolase is a convenient model system to study enzymatic thiamin catalysis. By using density functional theory (DFT) method, the transfer mechanism of a 2-carbon fragment between a donor ketose X5P and an acceptor aldose R5P catalyzed by transketolase has been studied on simplified models. The calculation results indicate that the whole reaction cycle contains several proton transfer processes as well as C—C bond formation and cleavage steps. Each C—C bond formation or cleavage step is always accompanied by a proton transfer process, which follows a concerted but asynchronous mechanism. The C—C bond formation is always prior to the proton transfer, and the C—C bond cleavage is always later than proton transfer, suggesting that the C—C bond ligation facilitates the proton transfer, and proton transfer promotes the C—C bond cleavage. In the first half- and second half-reactions, the energy barriers of C—C bond formations are always higher than those of C—C bond cleavages. The 4-amino group of cofactor ThDP and histidine residue can act as the proton donor/acceptor during the catalytic reaction.

1. Introduction

Transketolase (TK; EC 2.2.1.1) is an ubiquitous enzyme in cellular carbon metabolism, which requires thiamine diphosphate (ThDP), the biologically active form of vitamin B1, and Ca^{2+} ion as cofactors for enzymatic activity [1–4]. Transketolase was the first ThDP-dependent enzyme that yielded to a crystallographic structure analysis [5,6]. It catalyze the reversible transfer of a two-carbon fragment from a ketose to the C1 position of an aldose, as shown in Scheme 1 [7,8]. Transketolase is found in the non-oxidative branch of pentose phosphate pathway where it, together with transaldolase, creates a link to glycolysis. In plants and photosynthetic bacteria, TK is involved in the Calvin cycle where ribulose-1,5-bisphosphate is regenerated from phosphoglycerate [9]. In addition, recent studies show that TK appears to be an enzyme-crystallin [10] and promising drug target, and relates to the reduction of cancer growth [11] and alcohol-related brain damage [12].

In the past decades, the structures of TK from several species, including *Saccharomyces cerevisiae*, maize, *Escherichia coli*, *Leishmania mexicana*, *Bacillus anthracis* and *Francisella tularensis*, have been solved [5,13–15], and the high resolution (1.75 Å) crystal structure of human TK (PDB code: 3MOS), which was the first structure of a mammalian, has also been determined in 2010 [16]. These determinations of three-dimensional structures provide significant new insights into the fold of transketolases, binding mode of cofactors, and information of catalytic reaction. All TKs are homodimers and have two active sites of equal catalytic activity located at the dimer interfaces [7]. Based on these crystallographic and mutagenesis studies, a reaction cycle catalyzed by TK has been proposed [14,16], as shown in Fig. 1. The reaction mechanism can be divided into two half-reactions referred to as "ping-pong" mechanism. In the first half-reaction, the covalent donor-ThDP adduct (X5P–ThDP) is firstly formed by the attack of C_2 carbanion of ThDP ylide on the carbonyl of donor X5P (step 1), then the scissile $C_{2\alpha}$—$C_{3\alpha}$ bond of X5P–ThDP is broke to generate 1,2-dihydroxylethyl-ThDP (DHE-ThDP) carbanion/enamine intermediate and the first product G3P is liberated (step 2). In the second half-reaction, DHE-ThDP intermediate combines with the incoming second substrate R5P to yield S7P–ThDP adduct (step 3), which further undergoes a cleavage of C_2—$C_{2\alpha}$ to release the final product S7P and regenerate the ThDP ylide (step 4).

It is also noted that the amino acid sequences of TK from various sources are rather similar to each other [9,17]. For example, the transketolase from *E. coli* and humans show about 50% sequence identities to yeast enzyme [18–20].

Abbreviations: TK, transketolase; G3P, D-glyceraldehyde 3-phosphate; X5P, D-xylulose 5-phosphate; R5P, D-ribose 5-phosphate; S7P, D-sedoheptulose 7-phosphate; ThDP, thiamine diphosphate; DHE-ThDP, 1,2-dihydroxyethyl-ThDP; X5P–ThDP, covalent adduct of X5P and ThDP; S7P–ThDP, covalent adduct of S7P and ThDP.

* Corresponding author at: School of Chemistry and Chemical Engineering, Shandong University, Jinan, Shandong 250100, China. Tel.: +86 531 88365536; fax: +86 531 88564464.
E-mail address: yongjunliu_1@sdu.edu.cn (Y. Liu).

1093-3263/$ – see front matter © 2012 Elsevier Inc. All rights reserved.
http://dx.doi.org/10.1016/j.jmgm.2012.11.001

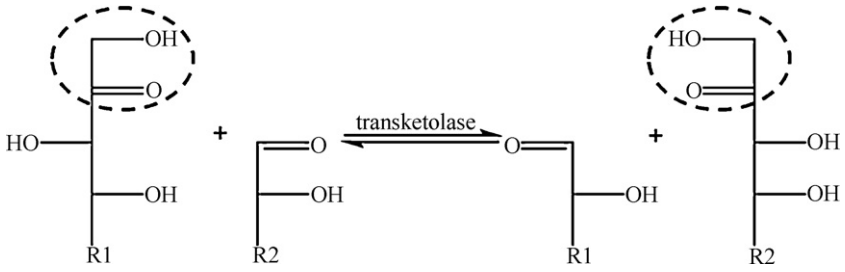

Scheme 1. The catalytic reaction of transketolase.

Further studies on the active sites of TKs from various organisms reveal that most of the active site residues are strictly conserved, and locate at almost the same position [17,21]. From the active center of human TK (Fig. 2), one can see that a cluster of histidines (His283/258/263 and His45/37/30 in TBTK/human TK/yeast TK with PDB codes 3RIM/3MOS/1NGS) and aspartic acid (Asp499/424/477) are involved in the formation of hydrogen bonds with the substrate hydroxyl groups, and another cluster of arginines (Arg378/318/359 and Arg552/474/528), histidine (His491/416/169) and serine (Ser405/345/386) are likely to bind with the phosphate group of the substrate [22]. The cofactor ThDP maintains in a so-called "V" configuration by the hydrogen bonds and hydrophobic interactions, which is proved to be an essential prerequisite for catalysis [2,5].

Many experimental advances have been made in understanding the catalytic mechanism of TK [4,15,17,22]. Up to now, the binding modes of ThDP and substrates, the activation mechanism of ThDP, the function of various active site residues, and some intermediates have been identified by using protein crystallography, site-directed mutagenesis and biochemical analysis [23–27]. The crystallographic and mutagenesis studies suggest that the histidine residues participate in the transition state stabilization and proton transfer [7,22,27,28]. In the first half-reaction, at least two proton transfer steps have to occur. The first proton transfer corresponds to the deprotonation of C2 carbon atom of the thiazolium of ThDP, which is common to all ThDP dependent enzymes. The second proton transfer occurs between the histidine residue and the $C_{3\alpha}$ hydroxyl group of the substrate (X5P), which is also common to the catalytic reaction of TK. In the second half-reaction, the proton transfer may occur between the histidine residue and the substrate (R5P). During these proton transfers, the cleavage and formation of C—C bonds may take place simultaneously or successively.

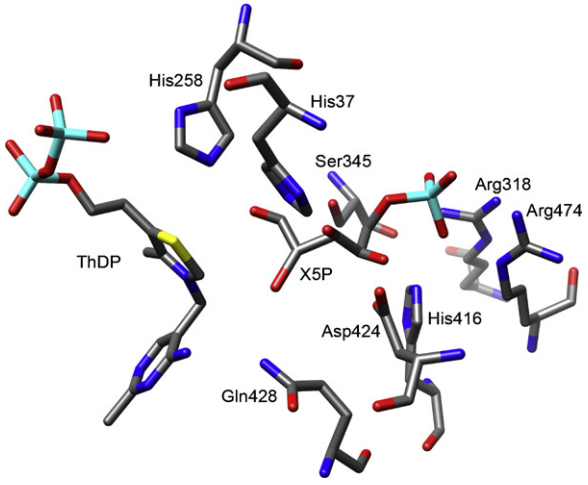

Fig. 1. Proposed catalytic mechanism of TK for the conversion of X5P and R5P yielding G3P and S7P.

Although a rough picture about the reaction mechanism of transketolase has been obtained, as described in a review article [7], open questions still remain. The detailed description of each individual step, the roles of pocket residues involved in proton transfer and stabilization of reaction intermediates and transition states, the energetics of the whole reaction and so on, are still not fully understood.

Several theoretical studies have focused on the catalytic mechanisms of some ThDP-dependent enzymes, such as pyruvate decarboxylase (PDC) [29–31], pyruvate ferredoxin oxidoreductase (PFOR) [32], and acetohydroxyacid synthase (AHAS) [33–35]. However, to our knowledge, the mechanistic research on the TK catalytic reaction using theoretical approaches is still very limited. In the present paper, the reaction mechanism of TK was investigated on simplified models with the aim to understand the common steps of TK catalysis by using hybrid density functional theory (DFT) method [36–41], which has been successfully used to study enzyme reaction mechanism [42]. The roles of pockets residues and the influences of protein environments on the energetics will be studied in the future by using QM/MM method.

2. Computational details

All calculations presented here were performed by using hybrid density functional theory method implemented in Gaussian 03 program package [43]. Geometrical structures were optimized at B3LYP/6-31G(d,p) level of theory. The X5P molecule was separately optimized and then deposited into the active pocket using the Autodock program [44]. To obtain more accurate energies, single point calculations on the optimized structures were performed with the larger basis set 6-311++G(2d,2p), which includes diffuse functions and double polarization functions on each atom. To consider the effects of enzyme environment on the energetics of each reaction step, we also used the polarizable-continuum model (PCM) [45,46] to calculate the single point energies at 6-311++G(2d,2p) level for each species on the optimized geometries. In this model, the solvent is represented by a constant dielectric medium surrounding a cavity containing the solute. The dielectric constant of the enzyme environment is chosen to be 4. Frequency calculations were performed with the 6-31G(d,p) basis set to obtain zero-point vibrational energies (ZPEs) and to confirm that all the optimized geometries correspond to a local minimum that has no imaginary frequency or a saddle point that has only one imaginary frequency. Since some atoms were frozen to their crystallographic positions, a few small negative eigenvalues usually appear, typically in the order of 10 cm^{-1}. These frequencies do not contribute significantly to the zero-point energies and can be ignored. All the transition states have been confirmed by intrinsic reaction coordinate (IRC) calculations.

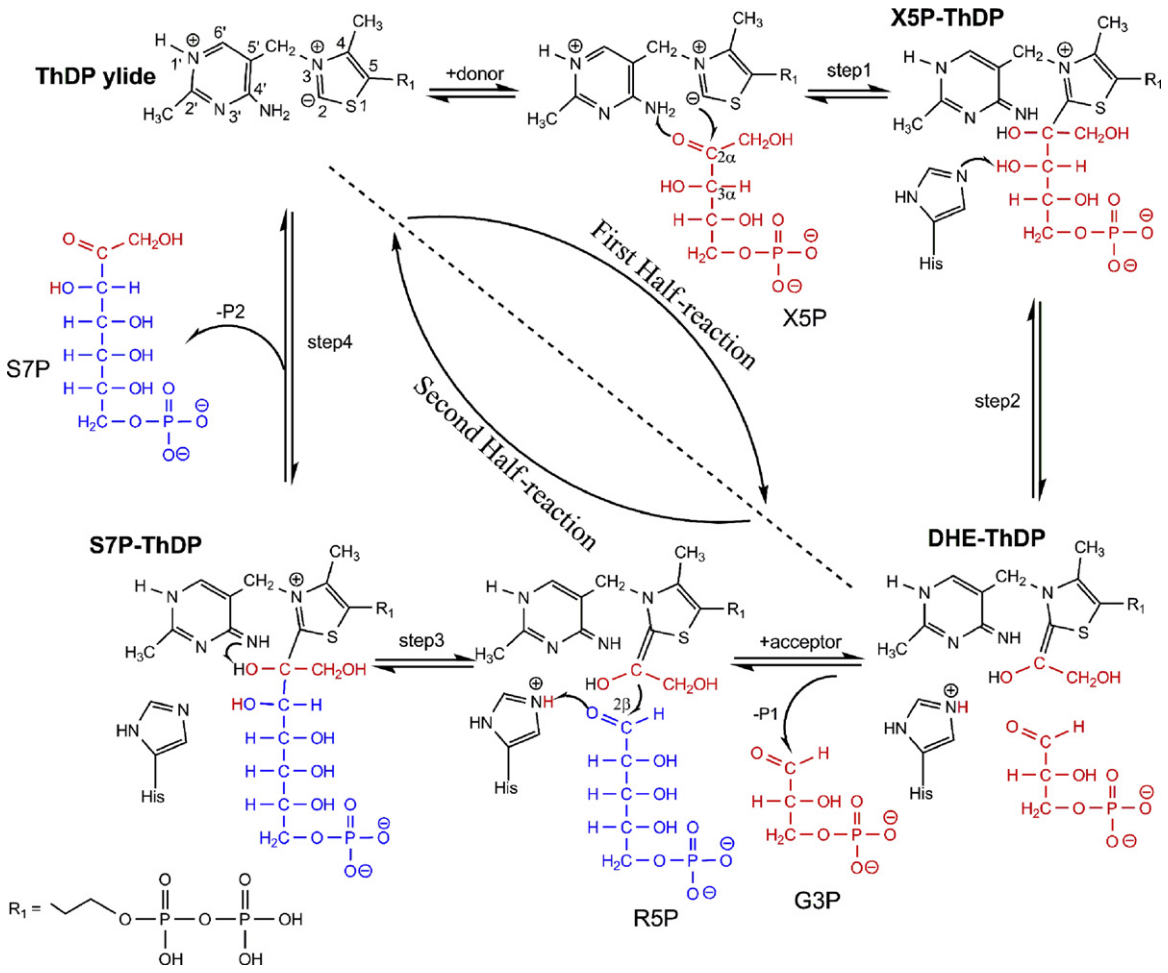

Fig. 2. Crystal structure of the active site of TK with the cofactor ThDP (PDB code 3MOS). The X5P molecule was separately optimized and then deposited into the active pocket using the autodock program.

3. Results and discussion

Since the activation mechanism of ThDP has been extensively studied elsewhere [29,47–50], our calculations start from a model that ThDP has been activated, i.e., the proton at the C2 carbon atom has been abstracted and the ThDP ylide has been formed. In addition, experimental studies show that the 4′-amino group of ThDP and the histidine residue (His258 in human TK, PDB code 3OOY) are directly involved in the catalytic reactions [22,27,28], the other residues mainly play a role in stabilizing the transition states and intermediates. Therefore, our models only consist of the truncated active form of ThDP (ThDP ylide), histidine residue His258 and substrates. As for the glutamate residue (Glu366 in human TK), Li et al have studied the effect of glutamate on the catalytic reaction of pyruvate decarboxylase by using different models [29]. They found that the barriers of ylide formation and product release processes decreased obviously if the glutamate residue was included. In this paper, the main aim is to study the reaction cycle after the activation of THDP. Therefore, to simplify the calculation, the glutamate residue was not included in our model. We can conjecture that the calculated energy barrier would be higher than that of the model with the presence of glutamate residue. During the optimizations, the truncated atoms were frozen to their crystallographic positions to prevent unrealistic movements of the groups involved in the model, and the fixed atoms were marked with asterisks in the corresponding figures. One can see that only few atoms were fixed in the model during the optimizations, including the terminal carbon atom of truncated residue His258 and the terminal carbon and oxygen atom of truncated ThDP. Although the strategy of ThDP freeze here is different from that adopted in earlier studies [29,31], it also can keep the V-like conformation of the ThDP in all species in the catalytic cycle. The characteristic torsion angles Φ_T and Φ_P for the orientation of the ThDP rings [51,52] in all species will be given in Figs. 3 and 5.

To clearly elucidate the whole catalytic cycle, the first half- and second half-reactions are discussed in the following sections, respectively.

3.1. First half-reaction

As shown in Fig. 1, in the first-half reaction, the intermediate X5P–ThDP and carbanion/enamine intermediate DHE-ThDP are formed successively. In our calculations, IM1 and IM2 are the simplified models of X5P–ThDP and DHE-ThDP, respectively. The optimized structures of initial reactant (R), transition states (TS1 and TS2) and intermediates (IM1 and IM2) are shown in Fig. 3.

From Fig. 3 one can see that in reactant (R) the histidine residue and the 4′-amino group of ThDP form two hydrogen bonds with the substrate X5P. The hydrogen bond length between the histidine residue and the $C_{3\alpha}$ hydroxyl group of the substrate is very short (r5, 1.83 Å), while that of the 4′-amino group of thiazole ring with the carbonyl oxygen atom of the substrate is long (r3, 2.81 Å).

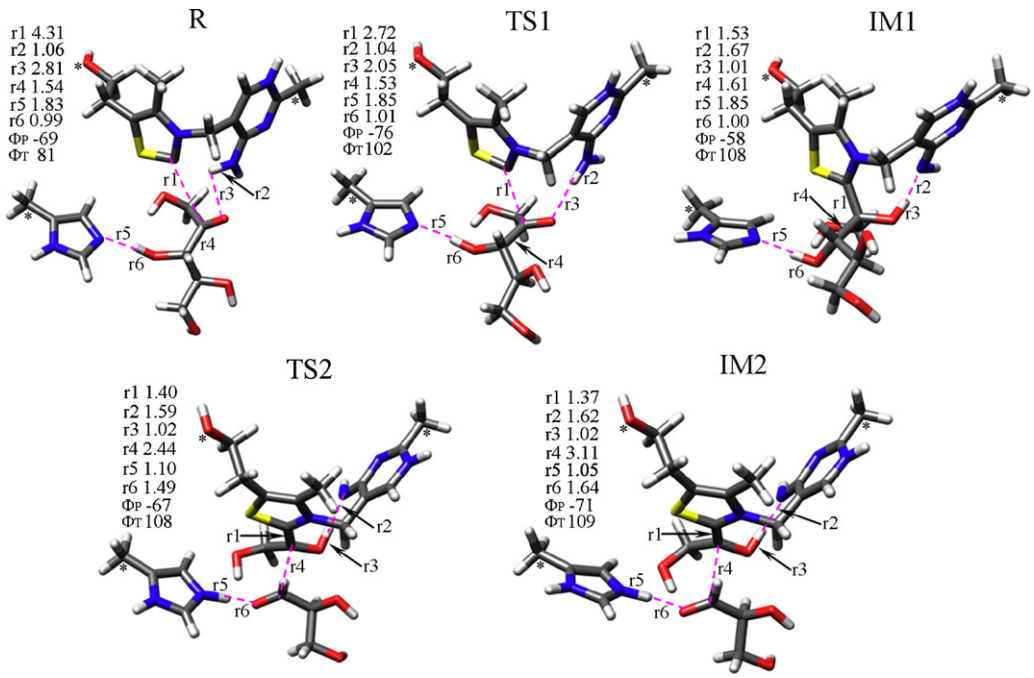

Fig. 3. Optimized geometries for various species in the first half-reaction obtained at the B3LYP/6-31g(d,p) level. The key bond distances are shown in angstrom and characteristic torsion angles Φ_T and Φ_P for the orientation of the ThDP rings are shown in degree. The fixed atoms are labeled by asterisks.

The C_2 carbanion of thiazole ring is far from the $C_{2\alpha}$ of the substrate (r1, 4.31 Å). In transition state (TS1), the C_2—$C_{2\alpha}$ distance changes to 2.72 Å (r1) from 4.31 Å, and the distance of hydrogen atom of 4′-amino group with the carbonyl oxygen atom changes to 2.05 Å (r3) from 2.81 Å. But the proton transfer from the 4′-amino group to the carbonyl oxygen does not start yet, i.e., the proton to be transfered is still at the 4′-amino group. In IM1, C_2—$C_{2\alpha}$ single bond is formed with distance of 1.53 Å (r1), and the proton transfer from the 4′-amino group to the carbonyl oxygen is completed. From the structures of R, TS1 and IM1, one can see that the ligation of C_2—$C_{2\alpha}$ bond and the proton transfer of hydrogen atom of 4′-amino group of ThDP is a concerted process but not precisely synchronous. The start of proton transfer is much later than the ligation of C_2—$C_{2\alpha}$ bond. In addition, the C_2—$C_{2\alpha}$ bond of X5P in IM1 is almost perpendicular to the thiazole ring of ThDP, which agrees well with the experimental observations [14].

The energy profile is shown in Fig. 4. To examine the effect of protein electrostatic surroundings on the energy barriers, the polarizable-continuum model (PCM) single point calculations at the level of 6-311++G(2d,2p) basis set were further performed on the optimized structures. The calculated energy barrier on the PCM model for the formation of IM1 is only 8.73 kcal/mol, implying the formation of IM1 is facile. The energy barrier in gas phase is 6.68 kcal/mol, indicating that the enzyme environment has a significant influence on the ligation step. The same effect was found in the other steps.

The next step is the cleavage of $C_{2\alpha}$—$C_{3\alpha}$ carbon bond of X5P–ThDP, and a proton transfer from the $C_{3\alpha}$ hydroxyl group of X5P to the proton acceptor (histidine residue) to generate DHE-ThDP carbanion/enamine intermediate IM2 and the first product G3P. From Fig. 3, one can see that in TS2 the $C_{2\alpha}$—$C_{3\alpha}$ carbon bond changes from 1.61 Å to 2.44 Å. Meanwhile, the proton of the $C_{2\alpha}$ hydroxyl group transfers to histidine residue, in which r5 changes from 1.85 to 1.10 Å. In IM2, the $C_{2\alpha}$—$C_{3\alpha}$ carbon bond (r4) changes to 3.11 Å, meaning the $C_{2\alpha}$—$C_{3\alpha}$ bond has broken. We also notes that this elementary reaction occurs in a concerted asynchronous mechanism, in TS2 the proton transfer is almost finished while the $C_{2\alpha}$—$C_{3\alpha}$ bond is on the way to be broken.

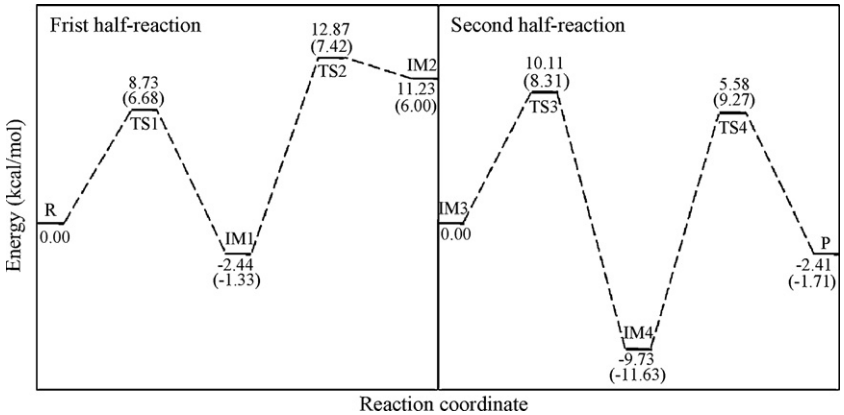

Fig. 4. Energy profile for the whole TK catalytic process. The ZPE-corrected relative energies obtained at the B3LYP/6-311++g(2d,2p)//B3LYP/6-31g(d,p) level in solution phase and gas phase (values in parentheses) are given in kcal/mol.

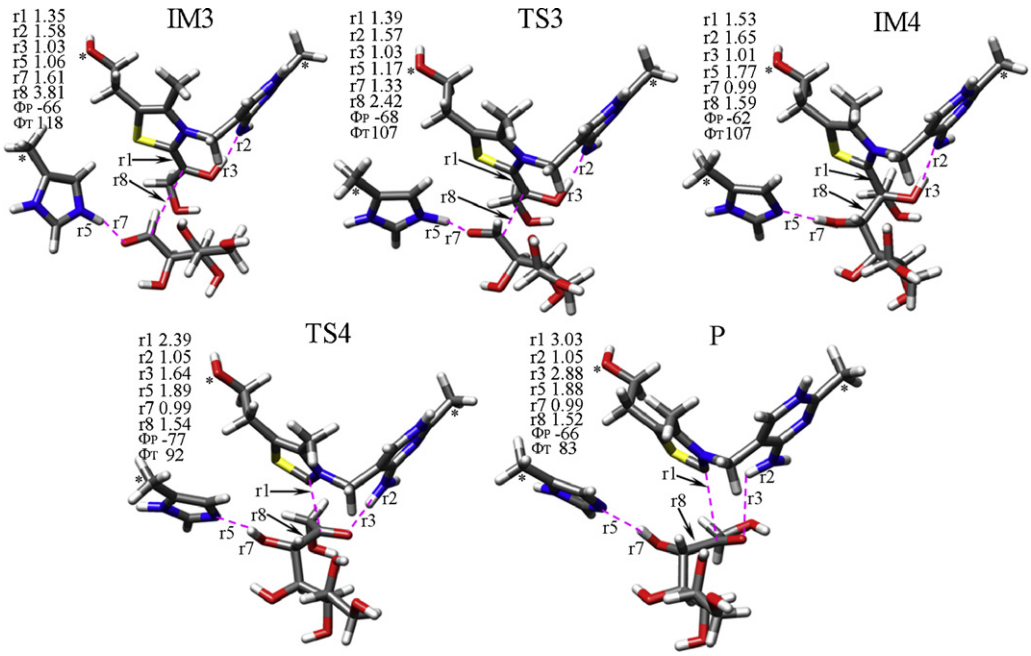

Fig. 5. Optimized geometries for various species in the second half-reaction obtained at the B3LYP/6-31g(d,p) level. The key bond distances are shown in angstrom and the characteristic torsion angles Φ_T and Φ_P for the orientation of the ThDP rings are shown in degree. The fixed atoms are labeled by asterisks.

From the energy point of view, we can see that the energy barrier for the formation of DHE-ThDP carbanion/enamine intermediate IM2 is higher than that of the formation of IM1 (15.31 vs. 8.73 kcal/mol). Moreover, the relative energy of IM2 is 13.67 kcal/mol higher than that of IM1, which means the reaction will stop at the first step and IM1 will be obtained if the second half-reaction could not occur. It agrees well with the experimental results of Asztalos et al. [14] that if only the donor substrate is present, TK catalysis is restricted to the donor half-reaction. Their intermediate studies on bacterial TK in the presence of 25 mM X5P showed that under equilibrium condition, 90% of active sites were occupied by X5P–ThDP, and no DHE-ThDP intermediate was observed [14]. Mitschke et al. [16] also observed that the fraction of the DHE-ThDP intermediate is too small (5% active sites) to allow a reliable quantitative analysis by NMR spectroscopy.

3.2. Second half-reaction

As shown in Fig. 1, the second-half reaction is the reversal of the first half-reaction. In the second half-reaction, the second substrate R5P reacts with the intermediate DHE-ThDP to form the intermediate S7P–ThDP, which further undergoes an another cleavage of C_2—$C_{2\alpha}$ carbon bond of S7P–ThDP and a proton transfer to generate the second product S7P and regenerate ThDP ylide.

In the first step (step 3 in Fig. 1), the acceptor R5P replaces the first product G3P, and complexes with the intermediate DHE-ThDP to form intermediate S7P–ThDP. By using the simplified model, the structures of transition state TS3 and intermediate IM4 were optimized, as shown in Fig. 5. The energy profile is shown in Fig. 4. It should be noted that IM4 is actually an analog of IM1, in which G3P is replaced by R5P. We can see that in the step to form intermediate IM4 (S7P–ThDP), the energy barrier is 10.11 kcal/mol, and the reaction energy is −9.73 kcal/mol, meaning S7P–ThDP is an even more stable intermediate, which agrees well with the experimental observation that the S7P–ThDP has been isolated successfully [16].

By checking the bonding distances (r8, r7 and r5), we found that the formation of C—C bond and proton transfer also follow a concerted asynchronous mechanism, in which the proton transfer is relatively later.

We also note that IM4 undergoes a higher energy barrier (18.31 kcal/mol) to generate the final product (S7P) and release the catalyst ThDP ylide. It is mainly due to that this step corresponds to the broken of C_2—$C_{2\alpha}$ carbon. The optimized structures in Fig. 5 indicates that, in TS4 the distance r2 is 1.05 Å, meaning the proton transfer from the $C_{2\alpha}$ hydroxyl group to the imine group of ThDP has been finished, while the distance r1 is 2.39 Å, implying the proton transfer process is prior to the cleavage of C_2—$C_{2\alpha}$ carbon bond.

4. Conclusions

The transfer mechanism of a two-carbon fragment between a donor ketose X5P and an acceptor aldose R5P catalyzed by transketolase has been studied by using density functional theory (DFT) method. The calculation results indicate that the whole reaction cycle contains four proton transfer steps, two C—C bond formation and two C—C bond cleavage processes. Each C—C bond formation or cleavage process is always accompanied by a proton transfer between the substrates and ThDP or histidine residue. In the first half- and second half-reactions, the energy barriers of C—C bond formations are always larger than that of C—C bond cleavages. The 4-amino group of cofactor ThDP and histidine residue play key roles in the proton transfer processes.

By comparing the energy barriers of four steps in gas phase and in enzymatic environment by using polarizable-continuum model (PCM), we found that the surrounding environment is crucial for this enzymatic reaction. These simplified models only provide us a rough picture of catalytic reaction, and the investigations that fully consider the effect of enzymatic environment are further deserved.

Acknowledgment

This work was supported by the Natural Science Foundation of China (21173129).

References

[1] R. Kluger, Thiamin diphosphate: a mechanistic update on enzymic and nonenzymic catalysis of decarboxylation, Chemical Reviews 87 (1987) 863–876.
[2] A. Schellenberger, Sixty years of thiamin diphosphate biochemistry, Biochimica et Biophysica Acta 1385 (1998) 177–186.
[3] R.A.W. Frank, F.J. Leeper, B.F. Luisi, Structure, mechanism and catalytic duality of thiamine-dependent enzymes, Cellular and Molecular Life Sciences 64 (2007) 892–905.
[4] F. Jordan, Current mechanistic understanding of thiamin diphosphate-dependent enzymatic reactions, Natural Products Reports 20 (2003) 184–201.
[5] Y. Lindqvist, G. Schneider, U. Ermler, M. Sundström, Three-dimensional structure of transketolase, a thiamine diphosphate dependent enzyme, at 2.5 Å resolution, EMBO Journal 11 (1992) 2373–2379.
[6] M. Nikkola, Y. Lindqvist, G. Schneider, Refined structure of transketolase from *Saccharomyces cerevisiae* at 2.0 Å resolution, Journal of Molecular Biology 238 (1994) 387–404.
[7] G. Schneider, Y. Lindqvist, Crystallography and mutagenesis of transketolase: mechanistic implications for enzymatic thiamin catalysis, Biochimica et Biophysica Acta 1385 (1998) 387.
[8] M.V. Kovina, G.A. Kochetov, Cooperativity and flexibility of active sites in homodimeric transketolase, FEBS Letters 440 (1998) 81–84.
[9] G. Schenk, R.G. Duggleby, P.F. Nixon, Properties and functions of the thiamin diphosphate dependent enzyme transketolase, International Journal of Biochemistry and Cell Biology 30 (1998) 1297–1318.
[10] C.M. Sax, C. Salamon, W.T. Kays, J. Guo, F.X. Yu, R.A. Cuthbertson, J. Piatigorsky, Transketolase is a major protein in the mouse cornea, Journal of Biological Chemistry 271 (1996) 33568–33574.
[11] L.G. Boros, J. Puigjaner, M. Cascante, W.N. Paul Lee, J.L. Brandes, S. Bassilian, F.I. Yusuf, R.D. Williams, P. Muscarella, W.S. Melvin, W.J. Schirmer, Oxythiamine and dehydroepiandrosterone inhibit the nonoxidative synthesis of ribose and tumor cell proliferation, Cancer Research 57 (1997) 4242–4248.
[12] K. Alexander-Kaufman, C. Harper, Transketolase: observations in alcohol-related brain damage research, International Journal of Biochemistry and Cell Biology 41 (2009) 717–720.
[13] S. Gerhardt, S. Echt, M. Busch, J. Freigang, G. Auerbach, G. Bader, W.F. Martin, A. Bacher, R. Huber, M. Fischer, Structure and properties of an engineered transketolase from maize, Plant Physiology 132 (2003) 1941–1949.
[14] P. Asztalos, C. Parthier, R. Golbik, M. Kleinschmidt, G. Hübner, M.S. Weiss, R. Friedemann, G. Wille, K. Tittmann, Strain and near attack conformers in enzymic thiamin catalysis: X-ray crystallographic snapshots of bacterial transketolase in covalent complex with donor ketoses cylulose 5-phosphate and fructose 6-phosphate, and in noncovalent complex with acceptor aldose ribose 5-phosphate, Biochemistry 46 (2007) 12037–12052.
[15] N.J. Veitch, D.A. Maugeri, J.J. Cazzulo, Y. Lindqvist, M.P. Barrett, Transketolase from *Leishmania mexicana* has a dual subcellular localization, Biochemical Journal 382 (2004) 759–767.
[16] L. Mitschke, C. Parthier, K. Schröeder-Tittmann, J. Coy, S. Lüdtke, K. Tittmann, The crystal structure of human transketolase and new insights into its mode of action, Journal of Biological Chemistry 285 (2010) 31559–31570.
[17] M. Sundström, Y. Lindqvist, G. Schneider, U. Hellman, H. Ronne, Yeast *TKL1* gene encodes a transketolase that is required for efficient glycolysis and biosynthesis of aromatic amino acids, Journal of Biological Chemistry 268 (1993) 24346–24352.
[18] G.A. Sprenger, U. Schörken, G. Sprenger, H. Sahm, Transketolase a of *Escherichia coli* K12, European Journal of Biochemistry 230 (1995) 525–532.
[19] B.A. McCool, S.G. Plonk, P.R. Martin, C.K. Singleton, Cloning of human transketolase cDNAs and comparison of the nucleotide sequence of the coding region in Wernicke-Korsakoff and non-Wernicke-Korsakoff individuals, Journal of Biological Chemistry 268 (1993) 1397–1404.
[20] E. Fullam, F. Pojer, T. Bergfors, T.A. Jones, S.T. Cole, Structure and function of the transketolase from *Mycobacterium tuberculosis* and comparison with the human enzyme, Open Biology 2 (2012) 110026.
[21] K. Tittmann, R. Golbik, K. Uhlemann, L. Khailova, G. Schneider, M. Patel, F. Jordan, D.M. Chipman, R.G. Duggleby, G. Hübner, NMR analysis of covalent intermediates in thiamin diphosphate enzymes, Biochemistry 42 (2003) 7885–7891.
[22] C. Wikner, U. Nilsson, L. Meshalkina, C. Udekwu, Y. Lindqvist, G. Schneider, Identification of catalytically important residues in yeast transketolase, Biochemistry 36 (1997) 15643–15649.
[23] O.A. Esakova, L.E. Meshalkina, R. Golbik, G. Hübner, G.A. Kochetov, Donor substrate regulation of transketolase, European Journal of Biochemistry 271 (2004) 4189–4194.
[24] M. Killenberg-Jabs, S. Köenig, I. Eberhardt, S. Hohmann, G. Hübner, Role of Glu51 for cofactor binding and catalytic activity in pyruvate decarboxylase from yeast studied by site-directed mutagenesis, Biochemistry 36 (1997) 1900–1905.
[25] G.A. Kochetov, I.A. Sevostyanova, Binding of the coenzyme and formation of the transketolase active center, IUBMB Life 57 (2005) 491–497.
[26] I.A. Sevostyanova, V.A. Selivanov, V.A. Yurshev, O.N. Solovjeva, S.V. Zabrodskaya, G.A. Kochetov, Cooperative binding of substrates to transketolase from *Saccharomyces cerevisiae*, Biochemistry (Moscow) 74 (2009) 789–792.
[27] V.A. Selivanov, M.V. Kovina, N.V. Kochevova, L.E. Meshalkina, G.A. Kochetov, Kinetic study of the H103A mutant yeast transketolase, FEBS Letters 567 (2004) 270–274.
[28] C. Wikner, L. Meshalkina, U. Nilsson, S. Bäckström, Y. Lindqvist, G. Schneider, His103 in yeast transketolase is required for substrate recognition and catalysis, European Journal of Biochemistry 233 (1995) 750–755.
[29] J.Y. Wang, H. Dong, S.H. Li, H.W. He, Theoretical study toward understanding the catalytic mechanism of pyruvate decarboxylase, Journal of Physical Chemistry B 109 (2005) 18664–18672.
[30] Q.Q. Hou, J. Gao, Y.J. Liu, C.B. Liu, A QM/MM study on the catalytic mechanism of pyruvate decarboxylase, Theoretical Chemistry Accounts 131 (2012) 1280.
[31] R. Friedemann, K. Tittmann, R. Golbik, G. Hübner, DFT and MP2 studies on the C_2—$C_{2\alpha}$ bond cleavage in thiamin catalysis, Journal of Molecular Catalysis B 61 (2009) 36–38.
[32] R.S. Assary, L.J. Broadbelt, Computatinal screening of novel thiamine-catalyzed decarboxylation reactions of 2-keto acids, Bioprocess and Biosystems Engineering 34 (2011) 375–388.
[33] J. Gonzalo, J. Verónica, V. Jordi, P. Xavier, D. Eduardo, B.A. Joel, A QM/MM study on the last steps of the catalytic cycle of acetohydroxyacid synthase, Computational and Theoretical Chemistry 966 (2011) 159–166.
[34] J. Gonzalo, J. Verónica, V. Jordi, P. Xavier, D. Eduardo, B.A. Joel, Computational study on the carboligation reaction of acetohydroxyacid synthase: new approach on the role of the $HEThDP^-$ intermediate, Proteins 78 (2010) 1774–1788.
[35] Y. Xiong, J.J. Liu, G.F. Yang, C.G. Zhan, Computational determination of fundamental pathway and activation barriers for acetohydroxyacid synthase-catalyzed condensation reactions of α-keto acids, Journal of Computational Chemistry 31 (2010) 1592–1602.
[36] A.D. Becke, Density-functional exchange-energy approximation with correct asymptotic behavior, Physical Review A 38 (1988) 3098–3100.
[37] A.D. Becke, Density-functional thermochemistry. I. The effect of the exchange-only gradient correction, Journal of Chemical Physics 96 (1992) 2155–2160.
[38] A.D. Becke, Density-functional thermochemistry. II. The effect of the Perdew–Wang generalized-gradient correlation correction, Journal of Chemical Physics 97 (1992) 9173–9177.
[39] A.D. Becke, Density-functional thermochemistry. III. The role of exact exchange, Journal of Chemical Physics 98 (1993) 5648–5652.
[40] C. Lee, W. Yang, R.G. Parr, Development of the Colle–Salvetti correlation-energy formula into a functional of the electron density, Physical Review B 37 (1998) 785–789.
[41] B. Miehlich, A. Savin, H. Stoll, H. Preuss, Results obtained with the correlation energy density functionals of Becke and Lee, Yang and Parr, Chemical Physics Letters 157 (1989) 200–206.
[42] M.A. Khan, R. Lo, T. Bandyopadhyay, B. Ganguly, Probing the reactivation process of sarin-inhibited acetylcholinesterase with α-nucleophiles: hydroxylamine anion is predicted to be a better antidote with DFT calculations, Journal of Molecular Graphics and Modelling 29 (2011) 1039–1046.
[43] M. Frisch, et al., Gaussian 03, Revision D.01, Gaussian Inc., Wallingford, CT, 2004.
[44] G.M. Morris, D.S. Goodsell, R.S. Halliday, R. Huey, W.E. Hart, R.K. Belew, A.J. Olson, Automated docking using a Lamarckian genetic algorithm and an empirical binding free energy function, Journal of Computational Chemistry 19 (1998) 1639–1662.
[45] V. Barone, M. Cossi, J. Tomasi, Geometry optimization of molecular structures in solution by the polarizable continuum model, Journal of Computational Chemistry 19 (1998) 404–417.
[46] J. Tomasi, M. Persico, Molecular interactions in solution: an overview of methods based on continuous distributions of the solvent, Chemical Reviews 94 (1994) 2027–2094.
[47] D. Kern, G. Kern, H. Neef, K. Tittmann, M. Killenberg-Jabs, C. Wikner, G. Schneider, G. Hübner, How thiamine diphosphate is activated in enzymes, Science 275 (1997) 67–70.
[48] G. Hübner, K. Tittmann, M. Killenberg-Jabs, J. Schäffner, M. Spinka, H. Neef, D. Kern, G. Kern, G. Schneider, C. Wikner, S. Ghisla, Activation of thiamin diphosphate in enzymes, Biochimica et Biophysica Acta 1385 (1998) 221–228.
[49] K. Tittmann, K. Mesch, M. Pohl, G. Hübner, K. Tittmann, K. Mesch, M. Pohl, G. Hübner, Activation of thiamine diphosphate in pyruvate decarboxylase from *Zymomonas mobilis*, FEBS Letters 441 (1998) 404–406.
[50] A. Bar-Ilan, V. Balan, K. Tittmann, R. Golbik, M. Vyazmensky, G. Hübner, Z. Barak, D.M. Chipman, Binding and activation of thiamin diphosphate in acetohydroxyacid synthase, Biochemitry 40 (2001) 11946–11954.
[51] Y.A. Muller, Y. Lindqvist, W. Furey, G.E. Schuza, F. Jordan, G. Schneider, A thiamin diphosphate binding fold revealed by comparison of the crystal structures of transketolase pyruvate oxidase and pyruvate decarboxylase, Structure 1 (1992) 93–103.
[52] Y.A. Muller, G.E. Schulz, Structure of the thiamine- and flavin-dependent enzyme pyruvate oxidase, Science 259 (1993) 965–967.